

University of Wollongong

Research Online

Australian Institute for Innovative Materials -
Papers

Australian Institute for Innovative Materials

1-1-2015

Anomalies in magnetoelastic properties of DyFe_{11.2}Nb_{0.8} compound

Jianli Wang

University of Wollongong, jianli@uow.edu.au

M F. Md Din

University of Wollongong, mfmd999@uowmail.edu.au

Shane J. Kennedy

ANSTO, Bragg Institute, Ansto, sjk@ansto.gov.au

Zhenxiang Cheng

University of Wollongong, cheng@uow.edu.au

Stewart J. Campbell

University of New South Wales, stewart.campbell@adfa.edu.au

See next page for additional authors

Follow this and additional works at: <https://ro.uow.edu.au/aiimpapers>



Part of the [Engineering Commons](#), and the [Physical Sciences and Mathematics Commons](#)

Research Online is the open access institutional repository for the University of Wollongong. For further information contact the UOW Library: research-pubs@uow.edu.au

Anomalies in magnetoelastic properties of DyFe_{11.2}Nb_{0.8} compound

Abstract

The structural and magnetic properties of DyFe_{11.2}Nb_{0.8} compound have been investigated by high intensity, high resolution synchrotron x-ray diffraction, ac magnetic susceptibility, and dc magnetization measurements as well as Mössbauer spectroscopy (5-300 K). The easy magnetization direction at room temperature is along the c-axis. With decreasing temperature, the magnetocrystalline anisotropy changes from easy-axis to easy-cone at T_{sr2} (~202 K), then to easy plane at T_{sr1} (~94 K). The thermal expansion coefficient obtained from the synchrotron x-ray study exhibits clear anomalies around both of the spin reorientation transition temperatures. The ⁵⁷Fe hyperfine interaction parameters and magnetic moments values have been determined for the 8i, 8j, and 8f sites from the Mössbauer spectra.

Keywords

2nb0, 8, dyfe11, compound, anomalies, properties, magnetoelastic

Disciplines

Engineering | Physical Sciences and Mathematics

Publication Details

Wang, J. L., Md Din, M. F., Kennedy, S. J., Cheng, Z. X., Campbell, S. J., Kimpton, J. A. & Dou, S. X. (2015). Anomalies in magnetoelastic properties of DyFe_{11.2}Nb_{0.8} compound. *Journal of Applied Physics*, 117 (17), 17C109-1-17C109-4.

Authors

Jianli Wang, M F. Md Din, Shane J. Kennedy, Zhenxiang Cheng, Stewart J. Campbell, Justin A. Kimpton, and S X. Dou

Anomalies in magnetoelastic properties of DyFe_{11.2}Nb_{0.8} compound

J. L. Wang,^{1,2,a)} M. F. Md Din,¹ S. J. Kennedy,² Z. X. Cheng,¹ S. J. Campbell,³
 J. A. Kimpton,⁴ and S. X. Dou¹

¹*Institute for Superconductivity and Electronic Materials, University of Wollongong, Wollongong, New South Wales 2522, Australia*

²*Bragg Institute, ANSTO, Lucas Heights, New South Wales 2234, Australia*

³*School of Physical, Environmental and Mathematical Sciences, The University of New South Wales, Canberra, Australian Capital Territory 2600, Australia*

⁴*Australian Synchrotron, 800 Blackburn Rd., Clayton 3168, Australia*

(Presented 6 November 2014; received 17 September 2014; accepted 18 October 2014; published online 5 February 2015)

The structural and magnetic properties of DyFe_{11.2}Nb_{0.8} compound have been investigated by high intensity, high resolution synchrotron x-ray diffraction, ac magnetic susceptibility, and dc magnetization measurements as well as Mössbauer spectroscopy (5–300 K). The easy magnetization direction at room temperature is along the c-axis. With decreasing temperature, the magnetocrystalline anisotropy changes from easy-axis to easy-cone at T_{sr2} (~202 K), then to easy plane at T_{sr1} (~94 K). The thermal expansion coefficient obtained from the synchrotron x-ray study exhibits clear anomalies around both of the spin reorientation transition temperatures. The ⁵⁷Fe hyperfine interaction parameters and magnetic moments values have been determined for the 8i, 8j, and 8f sites from the Mössbauer spectra. © 2015 AIP Publishing LLC.

<http://dx.doi.org/10.1063/1.4907614>

INTRODUCTION

RFe_{12-x}T_x compounds (R = rare-earth element) with the ThMn₁₂ structure (*I4/mmm* space group) exhibit a wide variety of magnetic behaviours [e.g., Refs. 1–3] and in recent decades have attracted significant interest due to their potential application as permanent magnets. As an example, they are found to exhibit different easy magnetization directions and spin-reorientation transitions depending on the rare-earth element.^{1,2} In RFe_{12-x}T_x compounds, the R atoms are located at the 2a site and the Fe atoms occupy three non-equivalent sites (8f, 8i, and 8j) with T atoms (if 3d) also sitting at 8i sites.^{1,3} For the DyFe_{12-x}T_x compounds, it is well accepted that the total magnetocrystalline anisotropy results from the contributions of both the Dy and Fe sublattices. The Fe-sublattice has a uniaxial magnetic anisotropy parallel to the c-axis whereas the Dy sublattice has basal-plane anisotropy, mainly as a consequence of the negative second-order Stevens coefficient of Dy³⁺.^{1,2} At low temperatures, the Dy-sublattice anisotropy is dominant but with increasing temperature the axial anisotropy of the Fe-sublattice becomes dominant, due to the rapid decrease in the Dy-sublattice anisotropy with increasing temperature.¹ The competing anisotropy contributions from the two sublattices can therefore lead to spin reorientation transitions. However, there exist some inconsistencies in the reported magnetic transitions for Dy(Fe,T)₁₂ compounds such as spin reorientation and first-order magnetization transition^{4,5}—Hu *et al.*⁴ suggested that a first-order spin reorientation takes place at T_{sr1} with a second-order spin reorientation occurring at T_{sr2},

while Andreev *et al.*⁵ reported two consecutive second-order spin reorientations at T_{sr1} and T_{sr2}.

In earlier work, we reported that DyFe_{12-x}Nb_x compounds with *x* = 0.55–0.85 (Ref. 6) have two spin-reorientation transitions below room temperature. The easy magnetization directions at room temperature are along the c-axis. With decreasing temperature, the magnetocrystalline anisotropy changes from easy axis to easy cone at T_{sr2}, then to easy plane at T_{sr1}. With increasing Nb content both T_{sr1} and T_{sr2} decrease monotonically but their Curie temperature T_C remains independent of Nb content.⁶ Similar behaviours were also observed in TbFe_{12-x}Ti_x systems⁷ where the spin reorientation temperatures are very sensitive to the Ti concentration (dT_{sr}/dx = -380 K/Ti) but T_C remain almost unchanged with variation in Ti content.

Recently, magneto-structural coupling has been found to play a critical role in many useful multifunctional properties, namely, giant magnetoresistance, magnetocaloric effect, and magnetostriction.⁸ While the magnetic properties of RFe_{12-x}T_x compounds have been reported in detail, relatively little attention has been paid to their magnetoelastic properties, especially in the regions around the spin reorientation temperatures. Here, we present a detailed investigation of the magnetic behaviours and magnetoelastic effects around the spin reorientation transitions in DyFe_{11.2}Nb_{0.8}.

EXPERIMENT

The DyFe_{11.2}Nb_{0.8} compound was synthesized under argon atmosphere by arc melting the constituent elements of purities at least 99.9%. The crystal structure of the sample was checked by high intensity x-ray powder diffraction ($\lambda = 0.7288 \text{ \AA}$; 80–300 K) at the Australian Synchrotron (AS).⁹

^{a)}Author to whom correspondence should be addressed. Electronic mail: jianli@uow.edu.au

The magnetization was measured in a magnetic field of 0.01 T over the temperature range from 5 K to 650 K using the vibrating sample magnetometer option of a Quantum Design 14 T physical properties measurement system (PPMS). The ac magnetic susceptibility was recorded using a conventional physical properties measurement system (PPMS-9, Quantum Design) over the temperature range of 5–340 K. The ^{57}Fe Mössbauer spectra were obtained between 5 K and 300 K using a standard constant acceleration spectrometer and a $^{57}\text{CoRh}$ source. The spectrometer was calibrated at room temperature with an α -iron foil.

RESULTS AND DISCUSSION

Figure 1(a) shows the synchrotron x-ray diffraction patterns of $\text{DyFe}_{11.2}\text{Nb}_{0.8}$ at 300 K and 80 K with details of the variable temperature patterns obtained around the (301) and (002) reflections over the spin reorientation transitions shown in the inset. Rietveld refinements of the x-ray diffraction data using the FULLPROF software confirm that $\text{DyFe}_{11.2}\text{Nb}_{0.8}$ crystallizes in the tetragonal ThMn_{12} structure (space group $I4/mmm$) and that the Nb atoms occupy the 8i site. The refinements also indicate that less than 6% of α -Fe and Fe_2Nb are present as impurity phases. As expected the crystal structure does not change with variation in temperature. The lattice parameters derived from the refinements are shown in Figure 1(b).

Analysis of the DC magnetization data (not shown here) leads to the Curie temperature of $T_C = 523(\pm 5)$ K with the two spin reorientation temperatures determined as $T_{\text{sr}1} = 202(\pm 2)$ K and $T_{\text{sr}2} = 94(\pm 2)$ K. As reported in our earlier work,¹⁰ there is strong magneto-structural coupling around T_C in $\text{RFe}_{12-x}\text{Nb}_x$ compounds where pronounced positive spontaneous volume magnetostriction has been observed below the Curie temperature. While Figure 1(b) reveals anomalies in the lattice parameters around both spin

reorientation temperatures, these structural changes are less pronounced than those observed at T_C .¹⁰ The structural changes around $T_{\text{sr}1} = 202$ K and $T_{\text{sr}2} = 94$ K are evident from the thermal expansion coefficients for $\text{DyFe}_{11.2}\text{Nb}_{0.8}$ shown in Figure 1(c).

It was found that in $\text{DyFe}_{11}\text{Ti}$ single crystal the spin-reorientation phase transitions and processes involving rotation of the magnetic moment strongly influence the temperature, field, and angular dependences of magnetostriction.¹¹ Given the equivalent crystal structure and similar magnetic behaviour, we assume that a similar mechanism exists in the $\text{DyFe}_{12-x}\text{Nb}_x$ system. With decreasing temperature, the Dy-sublattice anisotropy becomes dominant compared with the axial anisotropy of the Fe-sublattice, and the magnetic vector rotates away from the c -axis at $T_{\text{sr}2}$ to form a cone around the c -axis. With further decrease in temperature the cone angle, θ (between the easy magnetization direction and the four-fold axis [001]) increases smoothly to $T_{\text{sr}1}$ and exhibits an abrupt change up to 90° .⁶ Due to interaction of the anisotropic orbital electron cloud around the Dy^{3+} magnetic ion with the crystal field of the lattice, the strong magnetostructural coupling¹¹ can be reflected by the appearance of anomalies in the thermal expansion coefficients as observed here for $\text{DyFe}_{11.2}\text{Nb}_{0.8}$.

Figure 2(a) shows the temperature dependence of ac magnetic susceptibility under different DC fields. Comparisons of the warming and cooling runs reveal noticeable hysteresis effects around both spin reorientation transition temperatures, indicating first-order magnetic transitions. It is also noted that an applied DC magnetic field shifts both $T_{\text{sr}1}$ and $T_{\text{sr}2}$ to higher temperatures. For the present measurements, we use a fine powder sample which can be easily aligned to the easy direction (c -axis) by an applied magnetic field, so it can be assumed that the applied field is parallel to the c -axis. This agrees well with the behaviour reported in $\text{TbFe}_{11}\text{Ti}$ ⁷ where application of an external DC field shifts T_{sr} to higher

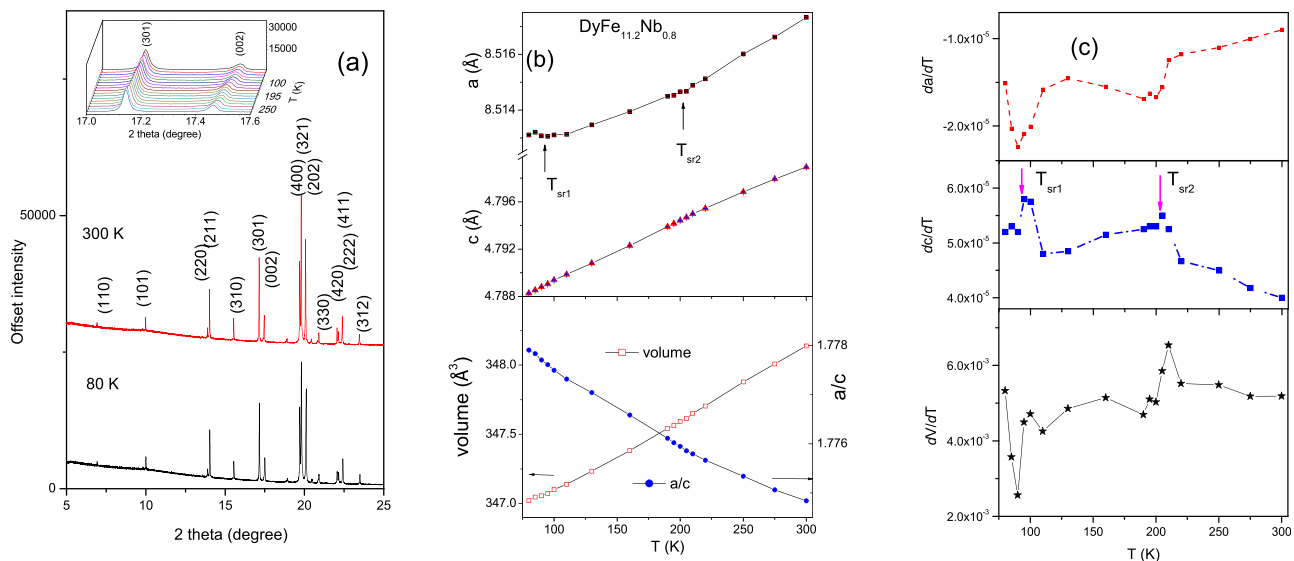


FIG. 1. (a) Synchrotron x-ray diffraction patterns of $\text{DyFe}_{11.2}\text{Nb}_{0.8}$ at 300 K and 80 K; the inset shows details of the patterns obtained for the 2θ region of the (301) and (002) reflections for temperatures over the spin reorientation transitions; (b) the lattice parameters of $\text{DyFe}_{11.2}\text{Nb}_{0.8}$ over the temperature range ~ 50 –300 K, and (c) the corresponding thermal expansion coefficients for $\text{DyFe}_{11.2}\text{Nb}_{0.8}$ as a function of temperature.

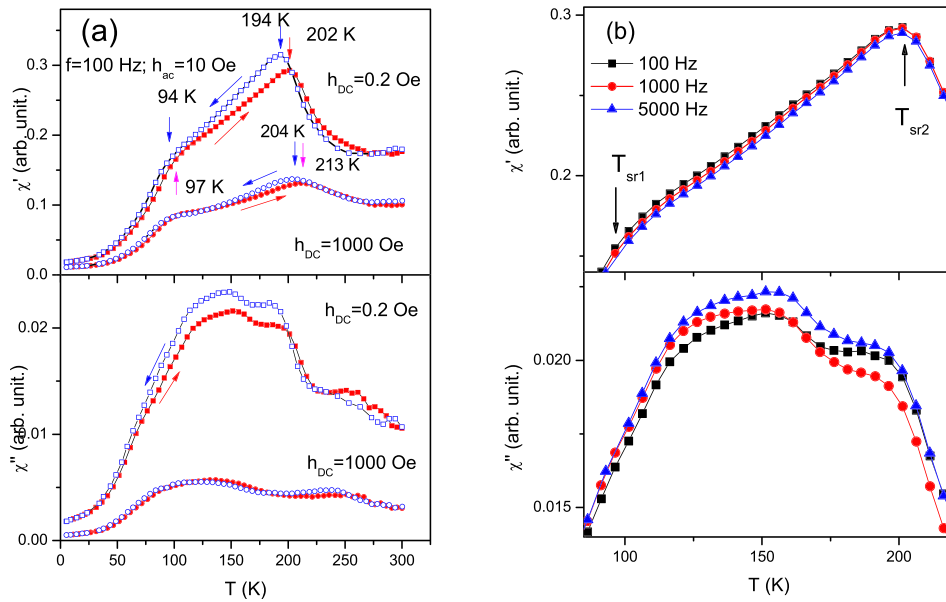


FIG. 2. Temperature dependences of the ac magnetic susceptibility of $\text{DyFe}_{11.2}\text{Nb}_{0.8}$ as measured under: (a) DC fields $h_{\text{DC}} = 0.2$ Oe ($h_{\text{ac}} = 10$ Oe; $f = 100$ Hz) and $h_{\text{DC}} = 1000$ Oe and (b) with different ac frequencies of $f = 100$ Hz, $f = 1000$ Hz, $f = 5000$ Hz ($h_{\text{ac}} = 10$ Oe; $h_{\text{DC}} = 0.2$ Oe; warming process). The warming (red) and cooling (blue) directions are indicated by arrows in Figure 2(a).

temperature with applied field parallel to the c -axis, while T_{sr} shifts down to lower temperature with field applied perpendicular to the (001) direction. The response of the spin reorientation transitions to ac susceptibility measurements at various ac frequencies is shown in Figure 2(b). No shift in spin reorientation temperature is obtained for T_{sr1} and T_{sr2} , while the amplitude of the imaginary parts of susceptibility exhibit a dependence on the exciting frequency. This is likely to be due to differing dynamic responses for different magnetic domains.

Mössbauer spectra have been collected at 5 K, 120 K, 150 K, 200 K, 270 K, and 300 K. The spectral features are very similar to those obtained for $\text{DyFe}_{11.4}\text{Nb}_{0.6}$ and are therefore not shown here. Details of the fitting procedure are as described previously.^{2,6} Similar to the behaviours reported for $\text{DyFe}_{11.4}\text{Nb}_{0.6}$ and $\text{ErFe}_{12-x}\text{Nb}_x$,² the overall shape of the spectrum changes with decreasing temperature as a result of the change in anisotropy. The temperature dependences of the hyperfine parameters are shown in Figure 3 with the spin reorientation transition temperatures marked by arrows. Based on the fact, the 8i sites are considered to provide the largest contribution to the overall 3d anisotropy,⁶ for clarity only the hyperfine field and quadrupole shift of the 8i sites are shown in Figure 3, in addition to the average values of the hyperfine parameters (full lines). It can be discerned from the trends of the data (dashed lines) that both the hyperfine field and quadrupole shift of the 8i sites exhibit a change around T_{sr2} . On the other hand, the lack of data points below T_{sr1} means that the expected anomaly around T_{sr1} is not evident as in the case for $\text{DyFe}_{11.4}\text{Nb}_{0.6}$ reported previously.⁶

Previously, it was reported that there exists a correlation between the ^{57}Fe isomer shift δ and the Wigner-Seitz cell (WSC) volume of the corresponding iron atoms in rare earth transition metal compounds with this correlation proving to be very successful in delineation of the electronic structure of these compounds.⁶ We have therefore calculated the WSC volumes with the BLOKJE program by using the structural and positional parameters in $\text{DyFe}_{11.2}\text{Nb}_{0.8}$ and the twelve-coordinated metallic radii of 1.8 Å, 1.26 Å, and 1.46 Å for Dy,

Fe, and Nb, respectively. The calculated WSC volumes for the 2a, 8i, 8j, and 8f sites at 300 K are 30.06 Å³, 12.76 Å³, 11.85 Å³, and 11.39 Å³, respectively. The isomer shifts behave as $\delta_{8i} > \delta_{8j} \approx \delta_{8f}$ at all temperatures (see Figure 3), which in general, correlates well with the WSC volumes.

The derived hyperfine fields for the 8i, 8j, and 8f sites at 5 K are 36.3 T, 30.7 T, and 26.4, respectively. While at

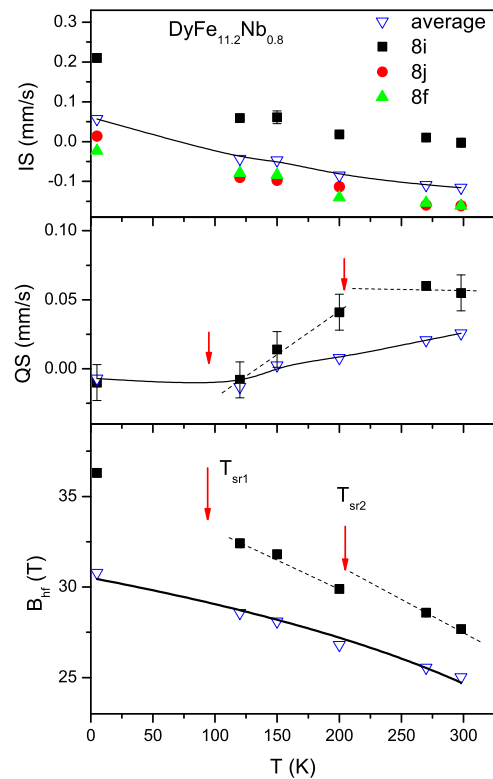


FIG. 3. Temperature dependence of the hyperfine parameters, quadrupole splitting, isomer shift, and magnetic hyperfine field for $\text{DyFe}_{11.2}\text{Nb}_{0.8}$. The full lines through the average values of the quadrupole splitting and isomer shift data are guides to the eye. The dashed lines show the trends of the quadrupole splitting and magnetic hyperfine fields of the 8i sites, while the solid line through the average hyperfine field values is the result of the fit as described in the text.

300 K, they change to 27.7 T, 25.1 T, and 22.8 T, respectively. If we assume the conversion factor (of $15.6 \text{ T}/\mu_{\text{B}}$) between the magnetization of the Fe sublattice with the corresponding hyperfine field [Ref. 6 and references therein] to be valid here, the magnetic moments values for the 8i, 8j, and 8f sites at 5 K have been determined to be $2.33 \mu_{\text{B}}$, $1.97 \mu_{\text{B}}$, and $1.69 \mu_{\text{B}}$, respectively. The temperature dependence of the average hyperfine field has been analysed in terms of power law¹² of the reduced temperature given by $B_{\text{hf}}/B_{\text{hf}}(0) = (1 - T/T_{\text{C}})^{\beta}$. The full line through the average values of the magnetic hyperfine field values in Figure 3 shows the resultant fit to this power law for $\text{DyFe}_{11.2}\text{Nb}_{0.8}$. The fitted exponent value of $\beta = 0.51(\pm 0.03)$ is close to the value obtained for mean field model corresponding to long range order which has a theoretical value of $\beta = 0.5$.¹³

CONCLUSIONS

The structural and magnetic properties of $\text{DyFe}_{11.2}\text{Nb}_{0.8}$ have been investigated over the temperature range of 5–300 K with particular interest focussing on the behaviour in the region of the spin reorientation temperatures $T_{\text{sr1}} = 202(\pm 2) \text{ K}$ and $T_{\text{sr2}} = 94(\pm 2) \text{ K}$. Our results show that anomalies in the thermal expansion coefficient correspond well with the spin reorientation temperatures. Temperature hysteresis in both spin reorientation temperatures has been detected indicating a first order nature for these transitions. A correlation between the ^{57}Fe isomer shift δ and the Wigner–Seitz cell volume has been shown to exist in $\text{DyFe}_{11.2}\text{Nb}_{0.8}$.

ACKNOWLEDGMENTS

This work was supported in part by grants from the Australian Research Council (Discovery Projects: DP0879070 and DP110102386).

- ¹B.-P. Hu, K.-Y. Wang, Y.-Z. Wang, Z.-X. Wang, Q.-W. Yan, P.-L. Zhang, and X.-D. Sun, *Phys. Rev. B* **51**, 2905 (1995).
- ²J. L. Wang, S. J. Campbell, J. M. Cadogan, O. Tegus, and A. V. J. Edge, *J. Phys.: Condens. Matter* **17**, 3689 (2005).
- ³D. I. Gorbunov, S. Yasin, A. V. Andreev, N. V. Mushnikov, E. V. Rosenfeld, Y. Skourski, S. Zherlitsyn, and J. Wosnitzer, *Phys. Rev. B* **89**, 214417 (2014); D. Sanavi Khoshnoud, N. Tajabor, L. Motevalizadeh, and D. Fruchart, *J. Magn. Magn. Mater.* **363**, 188 (2014).
- ⁴B. P. Hu, H. S. Li, J. P. Gavigan, and J. M. D. Coey, *J. Phys.: Condens. Matter* **1**, 755 (1989).
- ⁵A. V. Andreev, N. V. Kudrevatykh, S. M. Razgonyaev, and E. N. Tarasov, *Phys. B* **183**, 379 (1993).
- ⁶J. L. Wang, Y. P. Shen, C. P. Yang, N. Tang, B. Fuquan, D. Yang, G. H. Wu, and F. M. Yang, *J. Phys.: Condens. Matter* **13**, 1733 (2001); J. L. Wang, S. J. Campbell, J. M. Cadogan, S. James, and A. J. V. Edge, *Phys. Status Solidi C* **1**(12), 3377 (2004).
- ⁷J. L. Wang, G. H. Wu, N. Tang, D. Yang, F. M. Yang, F. R. de Boer, Y. Janssen, J. C. P. Klaasse, E. Bruck, and K. H. J. Buschow, *Appl. Phys. Lett.* **76**, 1170 (2000); J. L. Wang, B. García-Landa, C. Marquina, M. R. Ibarra, F. M. Yang, and G. H. Wu, *Phys. Rev. B* **67**, 014417 (2003).
- ⁸S. B. Roy, *J. Phys.: Condens. Matter* **25**, 183201 (2013) and references therein.
- ⁹K. S. Wallwork, B. J. Kennedy, and D. Wang, *AIP Conf. Proc.* **879**, 879 (2007).
- ¹⁰J. L. Wang, C. Marquina, B. García-Landa, M. R. Ibarra, F. M. Yang, and G. H. Wu, *Phys. B* **319**, 73 (2002).
- ¹¹S. A. Nikitin, I. S. Tereshina, and N. Yu. Pankratov, *Phys. Solid State* **41**, 1508 (1999).
- ¹²M. Venkatesan, U. V. Varadaraju, and K. V. S. Rama Rao, *Phys. Rev. B* **64**, 094427 (2001); J. Chi, Y. Li, F. G. Vagizov, V. Goruganti, and J. H. Ross, Jr., *ibid.* **71**, 024431 (2005).
- ¹³S. N. Kaul, *J. Magn. Magn. Mater.* **53**, 5 (1985).